

Determining the Supernova Direction by its Neutrinos

Shinichiro Ando^a and Katsuhiko Sato^{a,b}

^a*Department of Physics, University of Tokyo, 7-3-1 Hongo, Bunkyo,
Tokyo 113-0033, Japan*

^b*Research Center for the Early Universe, University of Tokyo,
7-3-1 Hongo, Bunkyo, Tokyo 113-0033, Japan*

February 8, 2020

Abstract

Supernova neutrinos which arrive at the earth earlier than the light enable us the earliest determination of the direction of their emitter supernova. The theme of this paper is how accurately we can determine the supernova direction. We simulate supernova neutrino events at SuperKamiokande detector, using a realistic supernova model and several realistic neutrino oscillation models. In SuperKamiokande detector, the electron scattering reactions ($\nu + e^- \rightarrow \nu + e^-$) are highly correlated to the injected neutrinos' direction. These reactions, in the large background of isotropic inverse β -decay reactions ($\bar{\nu}_e + p \rightarrow e^+ + n$), are key to determine the supernova direction. As a result of our simulation we can restrict the supernova direction to be within a circle of radius 10° . Especially in several neutrino oscillation models, this accuracy is enhanced to 8° .

1 Introduction

If we want to obtain the information about the core-collapse supernova explosion, which is rare in the Galaxy [1], it is very important to observe the light curve of its early phase. A future core-collapse supernova explosion in our Galaxy is expected to be detected by several neutrino detectors around the world. When it occurred, neutrinos produced in the core can escape from the supernova immediately, because of their very weak interaction with matter. On the other hand, photons do not get out until the shock wave travels from the core through the stellar envelope and breaks out of the stellar photosphere. So we can catch the neutrino signal several hours earlier than the light. (Of course this time delay depends on the size of the envelope (Ref. [2] contains a simple model of this delay).) In addition, because the electromagnetic signals are obscured by dust in the interstellar space, it is plausible that we cannot find the supernova explosion without the neutrino signal. So, if we could determine the direction of the supernova explosion by its neutrinos, a lot of astronomical observations of its early state would be possible. In fact, world-wide early supernova alert project is running (SNEWS, or SuperNova Early Warning System). [3, 4]

This problem (of determining the supernova direction by its neutrinos) has been discussed in general before [5]-[9]. There are two methods to deal with this problem. The first technique is using the angular distributions of the neutrino reaction products, which can be correlated with the supernova direction. The result of this approach by the past work is rather optimistic (for example, in Ref. [5], $\delta\theta \simeq 5^\circ$ for SuperKamiokande, and $\delta\theta \simeq 20^\circ$ for SNO), based on rather qualitative discussions. The second method is based

on triangulation using two or more widely-separated detectors. But this technique was shown to be very crude in Ref. [5] ($\delta \cos \theta \simeq 0.5$ for SuperKamiokande and SNO), contrary to the former optimistic estimate in, for example, Ref. [6].

In this paper, we simulate a supernova explosion in the Galactic plane ($D = 10$ kpc as used in Ref. [5], for comparison) and discuss the statistical error of its direction according to the first method above. In addition, we also consider the more realistic case, or “neutrino oscillation”, which is supported by solar [10]-[12] and atmospheric neutrino [13] data. This realistic case, however, was not considered in the previous works. We expect that in the case of the neutrino oscillation the accuracy of the supernova direction becomes better, since the energy of ν_e 's, which have the largest contribution of determining the direction, is enhanced due to the conversion “ $\nu_e \leftrightarrow \nu_{\mu,\tau}$.” (Because $\nu_{\mu,\tau}$'s experience only neutral-current reactions in the supernova and weakly interact with matter compared to ν_e 's, $\nu_{\mu,\tau}$'s reach the equilibrium at deeper in the core than ν_e 's and their temperatures are higher than ν_e 's.)

The construction of this paper is as follows: In Section 2, a realistic supernova model and neutrino oscillation models used in the simulation are illustrated. Reactions at SuperKamiokande detector and these cross sections are discussed in Section 3. Based on these models and reactions, we simulate a supernova explosion in our Galaxy and events at SuperKamiokande in Section 4. A detail of this simulation and its results about the accuracy of the direction are also shown in this section. Finally we discuss about our results in Section 5.

2 Supernova Model and Oscillation Parameters

We use a realistic model of a collapse-driven supernova by the Lawrence Livermore group [14]. Time-integrated energy spectra for a no oscillation case is shown in Fig. 1.(See Ref. [15] for detail.) In this model, however, the radiation of neutrinos is isotropic, contrary to the fact that supernova progenitors are rotating, which many observations have indicated, and they radiate anisotropic neutrinos [16]. For now, we don't consider the effect of rotation for simplicity.

We use four models of neutrino mixing parameters used in Ref. [17] (see Table 1) and the results of the supernova neutrino oscillation in [17] is also used. Of course these models are made to agree with the results of the solar and the atmospheric neutrinos [10]-[13]. “LMA” and “SMA” indicate MSW solution of the solar neutrino problem. Recent SNO observation [12], with other observations, shows that LMA solution are more favorable but SMA solution are not allowed until 3σ level (see Ref. [18] and references therein). However, we also deal with SMA solution for comparison. “-L” and “-S” indicate whether θ_{13} is large or small. A large (small) θ_{13} means “higher resonance” is adiabatic (nonadiabatic). The adiabatic higher resonance enhances the energy of the electron neutrinos, and enhances the event rate of ν_e scattering which indicate good dependence on the supernova direction (see below). For the review of MSW effect, see Ref. [19].

3 Expected Events in SuperKamiokande

SuperKamiokande(SK) is a water Čerenkov detector with 32,000 ton pure water based at Kamioka in Japan. The relevant interactions of neutrinos with water are as follows:

$$\bar{\nu}_e + p \rightarrow n + e^+ \quad (\text{CC}) \quad (1)$$

$$\nu_e + e^- \rightarrow \nu_e + e^- \quad (\text{CC and NC}) \quad (2)$$

$$\bar{\nu}_e + e^- \rightarrow \bar{\nu}_e + e^- \quad (\text{CC and NC}) \quad (3)$$

$$\nu_{\mu,\tau}(\bar{\nu}_{\mu,\tau}) + e^- \rightarrow \nu_{\mu,\tau}(\bar{\nu}_{\mu,\tau}) + e^- \quad (\text{NC}) \quad (4)$$

$$\nu_e + O \rightarrow F + e^- \quad (\text{CC}) \quad (5)$$

$$\bar{\nu}_e + O \rightarrow N + e^+ \quad (\text{CC}), \quad (6)$$

where CC and NC stand for charged current and neutral current interactions, respectively.

The efficiency of SK detector is 100% for an electron which energy is above 5 MeV and 50% at 4.2 MeV. For the energy and the angular resolution of SK, we refer to [20]. The energy resolution is $\sim 15\%$ for an electron with energy 10 MeV. We show the angular resolution as a function of the recoil electron energy in Fig. 2. In that figure we fitted experimental data to the function $83^\circ(E_e/\text{MeV})^{-0.5}$, which is used in our simulation.

For the differential cross section of the electron scattering (2)-(4), we refer to Ref. [21],

$$\frac{d\sigma}{d\cos\theta} = \frac{G_F^2 T_e^2 (1 + 2m_e/T_e)^{3/2}}{2\pi (1 + m_e/E_\nu)} \left[A + B \left(1 - \frac{T_e}{E_\nu}\right)^2 + C \frac{m_e T_e}{E_\nu^2} \right] \quad (7)$$

$$\cos\theta = \frac{E_\nu + m_e}{E_\nu} \left(\frac{T_e}{T_e + 2m_e} \right)^{1/2}, \quad (8)$$

where T_e is the electron kinetic energy, E_ν is the neutrino energy, and the coefficients

A , B , and C are shown in Table.2. This differential cross section is highly forward peaked as shown in Fig. 3. Further with threshold energy (5 MeV), the forward peak is enhanced.

For the differential cross section of $\bar{\nu}_e p$ CC reaction (1), we refer to Ref. [22],

$$\frac{d\sigma}{d\cos\theta} = \frac{\sigma_0}{2} \left[(f^2 + 3g^2) + (f^2 - g^2) \cos\theta - \frac{\Gamma}{M} \right] E_e^{(0)} E_e^{(0)} \quad (9)$$

$$\begin{aligned} \Gamma &= 2(f + f_2)g[(2E_e^{(0)} + \Delta)(1 - \cos\theta)] + (f^2 + g^2)[\Delta(1 + \cos\theta)] \\ &+ (f^2 + 3g^2)[3(E_e^{(0)} + \Delta)(1 - \cos\theta) - \Delta] \\ &+ (f^2 - g^2)[3(E_e^{(0)} + \Delta)(1 - \cos\theta) - \Delta] \cos\theta, \end{aligned} \quad (10)$$

where $f = 1$, $g = 1.26$, and $f_2 = \mu_p - \mu_n = 3.706$. M is the nucleon mass, and $\Delta = M_n - M_p$. The normalizing constant σ_0 , including the energy-independent inner radiative corrections, is

$$\sigma_0 = \frac{G_F^2 \cos^2 \theta_C}{\pi} (1 + \Delta_{inner}^R), \quad (11)$$

where $\Delta_{inner}^R \simeq 0.024$. This cross section (9) is taken to the first order of E_ν/M , and depend on the zeroth order positron energy $E_e^{(0)} = E_\nu - \Delta$. As shown in Fig. 4, the differential cross section of the $\bar{\nu}_e p$ reaction is almost isotropic. And the $\bar{\nu}_e p$ reaction has the largest contribution to the detected events at SK (e.g. at $E_\nu = 10$ MeV, $\sigma(\bar{\nu}_e p) \simeq 100\sigma(\nu_e e^-)$). So, it is not easy to see the peak position of events, of which information enables us to determine the supernova direction easily.

The differential cross section of the reactions with the oxygen (5),(6) is unclear, because of the uncertainty of the the nuclear part. These reactions are important if we consider the case with ‘‘neutrino oscillation’’, because the oscillation enhances the energy of ν_e and $\bar{\nu}_e$ which contribute to the reactions with the oxygen, and therefore enhances the

cross sections of these reactions. The differential cross sections with oxygen calculated in Ref. [23] are highly backward peaked when the neutrino energy becomes larger, so the reactions with the oxygen seem to be useful for determining the supernova direction. However, the backward peak of these reactions are not as sharp as the forward peak of the electron scattering reactions. Therefore we don't consider the reactions with the oxygen, because we guess that these reactions hardly influence the result without them.

The number of events at SK was calculated in Ref. [17] when the supernova exploded at $D = 10$ kpc. We show these results in Table 3 (cf: reactions with oxygen are also shown).

In SNO, we cannot expect the better accuracy of the direction than SK (see Ref. [5], for example). So, we don't discuss the events in SNO.

4 Simulation and Results

We assume that the supernova explosion occurred at $D = 10$ kpc. To get the information about the direction of the supernova, we have to set the coordinate at SK. Here, we set z -axis to the upward-direction. And we use spherical coordinate (θ, ϕ) as follows to determine the direction:

$$x = \cos \theta \sin \phi \tag{12}$$

$$y = \sin \theta \sin \phi \tag{13}$$

$$z = \cos \theta. \tag{14}$$

We also assume here that the direction of the supernova is $(\theta, \phi) = (135^\circ, 270^\circ)$. In

this case, the peak position should be $(\theta, \phi) = (45^\circ, 90^\circ)$. (Of course when we analyze the events, we must not use this peak information.)

First, we consider the case of “no oscillation”.

We show in Fig. 5 the distribution of the events. There seems to be the obscure peak around $(\theta, \phi) = (45^\circ, 90^\circ)$. To analyze this result systematically, we divide $\cos \theta$ direction in 20 bins and sum up in each bin. Fig. 6 is the result of this operation. The dashed line in Fig. 6 is $\theta = 0^\circ$ peaked case, which can easily be calculated theoretically with cross sections.

Then, we rotate the coordinate for the events to be seen as in the case of $\theta = 0^\circ$ peaked by using the least-square method. Best-fitted result is shown in Fig. 7. This result is obtained at coordinate rotation angle $(\theta, \phi) = (47.7^\circ, 80.0^\circ)$.

This result is near the “true” value $(45^\circ, 90^\circ)$, but this only one simulation is not sufficient to estimate the errors. So, we simulated 1,000 times under the same condition and obtained the distribution of the best-fitted coordinate rotation angle. Fig. 8 and Fig. 9 are the distributions of the best-fitted rotation angles, θ and ϕ , respectively. We fitted these results to Gaussian. These one sigma errors are $(\delta\theta, \delta\phi) = (6.8^\circ, 10.0^\circ)$. The one sigma error in two-dimensions is $\sigma = (\delta\theta^2 + \sin^2 \theta_0 \delta\phi^2)^{1/2} = 9.9^\circ$. Then in this method we can determine the supernova direction with $\sigma = 9.9^\circ$.

We adopted the same simulations to the other four “neutrino oscillation” cases. We summarize these results in Table 4.

5 Discussion

As shown in Table 4, we can determine the supernova direction within $\sim 10^\circ$. In the five models with which we dealt in this paper, “LMA-L” and “SMA-L” are better, because the electron scattering events are more prominent as shown in Table 3.

Now we further discuss on two points below, where we assume “no oscillation”.

5.1 Oxygen Events

As discussed above and shown in Table 3, we must consider the oxygen events, especially in the case of “neutrino oscillation”. We don’t expect that these effects enables us to determine the direction more accurately than the no oscillation case. Rather, for their reaction cross sections are unclear, they may disturb our analyses as noises.

If we would like to know the supernova direction without the oxygen which is really complex, it is one method to include “energy cut-off”. For example, we only see the electrons whose energy is under 15 MeV, so that we expect that the oxygen events have little contribution. (But we cannot be confident that this energy cut-off (15 MeV) is really enough.) With this energy cut-off, we simulated in the same way. In result, the accuracy is rather worse, $\sigma \sim 15^\circ$. This is because lower energy electrons (positrons) are scattered off in the detector and that makes the angular resolution of these electrons (positrons) worse as shown in Fig. 2.

5.2 Dependence on Distance

The simulation and its results we have shown above are based on the assumption that the supernova exploded at distance $D = 10$ kpc. We also simulated assuming other distance ($D = 5, 7.5, 12.5, 15, 17.5, 20$ kpc) and fitted their results as a function of the distance, as follows:

$$\sigma \simeq 8.9^\circ \left(\frac{D}{10\text{kpc}} \right). \quad (15)$$

This result is illustrated naively as follows: The event number at the earth falls off as the distance D squared, $N \propto D^{-2}$, and the accuracy σ is proportional to $1/\sqrt{N}$. Then, we expect that the accuracy is proportional to the distance.

6 Acknowledgments

We would like to thank SuperKamiokande people including Y. Fukuda for useful discussions, and also would like to thank K. Takahashi for preparing the numerical data of the neutrino oscillation and for useful discussions. This work was supported in part by Grants-in-Aid for Scientific Research provided by the Ministry of Education, Science and Culture of Japan through Research Grant No.07CE2002.

References

- [1] R.A. Muller et al., *Astrophys. J.* 384 (1992) L9; S. van den Bergh, *Comments Astrophys.* 17 (1993) 125; G.A. Tammann, W. Löffler, A. Schröder, *Astrophys. J. Suppl.* 92 (1994) 487; F.X. Timmes, R. Diehl, and D.H. Hartmann, *Astrophys. J.* 479 (1997) 760.

- [2] S.E. Woosley, P.A. Pinto, P.G. Martin, and Thomas A. Weaver, *Astrophys. J.* 318 (1987) 664; T. Shigeyama, K. Nomoto, M. Hashimoto, and D. Sugimoto, *Nature* 328 (1987) 320.
- [3] K. Scholberg, astro-ph/9911359.
- [4] A. Habig, for the SNEWS Collaboration, astro-ph/9912293.
- [5] J.F. Beacom and P. Vogel, *Phys. Rev. D* 60 (1999) 033007.
- [6] A. Burrows, D. Klein, and R. Gandhi, *Phys. Rev. D* 45 (1992) 3361.
- [7] G.V. Domogatsky and G.T. Zatsepin, in *Proceedings of the 9th International Conference on Cosmic Rays, Vol. 2* (Institute of Physics and the Physics Society, London, 1966), p. 1030.
- [8] A.A. Belyaev, Yu.S. Kopysov, O.G. Ryazhskaya, and G.T. Zatsepin, in *Neutrinos-78*, edited by E.C.Fowler (Purdue University, West Lafayette, IN, 1978), p. 871.
- [9] F.M. LoSecco, *Science* 224 (1984) 56.
- [10] S. Fukuda et al., *Phys. Rev. Lett.* 86 (2001) 5656.
- [11] J.N. Bahcall, P.I. Krastev, and A.Yu. Smirnov, *Phys. Rev. D* 58 (1998) 096016.
- [12] Q.R. Ahmad et al., SNO Collaboration, nucl-ex/0106015.
- [13] Y. Fukuda et al., *Phys. Rev. Lett.* 82 (1999) 2644; I. Scholberg, hep-ex/9905016.

- [14] J.R. Wilson, R. Mayle, S. Woosley, and T. Weaver, *Ann. NY Acad. Sci.* 470 (1986) 267.
- [15] T. Totani, K. Sato, H.E. Dalhed, and J.R. Wilson, *Astrophys. J.* 496 (1998) 216.
- [16] T.M. Shimizu, T. Ebisuzaki, K. Sato, and S. Yamada, *Astrophys. J.* 552 (2001) 756.
- [17] K. Takahashi, M. Watanabe, K. Sato, and T. Totani, hep-ph/0105204.
- [18] P.I. Krastev and A.Yu. Smirnov, hep-ph/0108177.
- [19] T.K. Kuo and J. Pantaleone, *Rev. Mod. Phys.* 61 (1989) 937.
- [20] M. Nakahata et al., *Nucl. Instrum. Methods A*421 (1999) 113.
- [21] M. Fukugita, A. Suzuki, *Physics and Astrophysics of Neutrinos* (Springer-Verlag, Tokyo, 1994).
- [22] P. Vogel and J.F. Beacom, *Phys. Rev. D* 60 (1999) 053003.
- [23] W.C. Haxton, *Phys. Rev. D* 36 (1987) 2283.

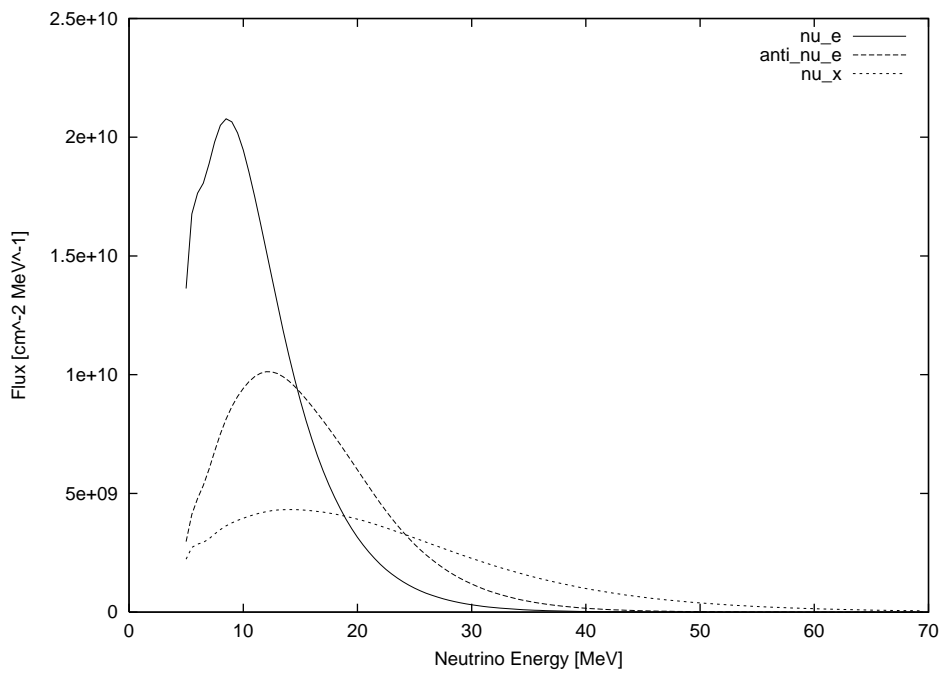


Figure 1: Energy spectra of ν_e , $\bar{\nu}_e$ and ν_x of the numerical supernova model used in this paper(, where ν_x means $\nu_{\mu,\tau}$ and $\bar{\nu}_{\mu,\tau}$). The solid, dashed and dotted lines are the spectrum of ν_e , $\bar{\nu}_e$ and ν_x , respectively. These spectra are assumed “no oscillation”

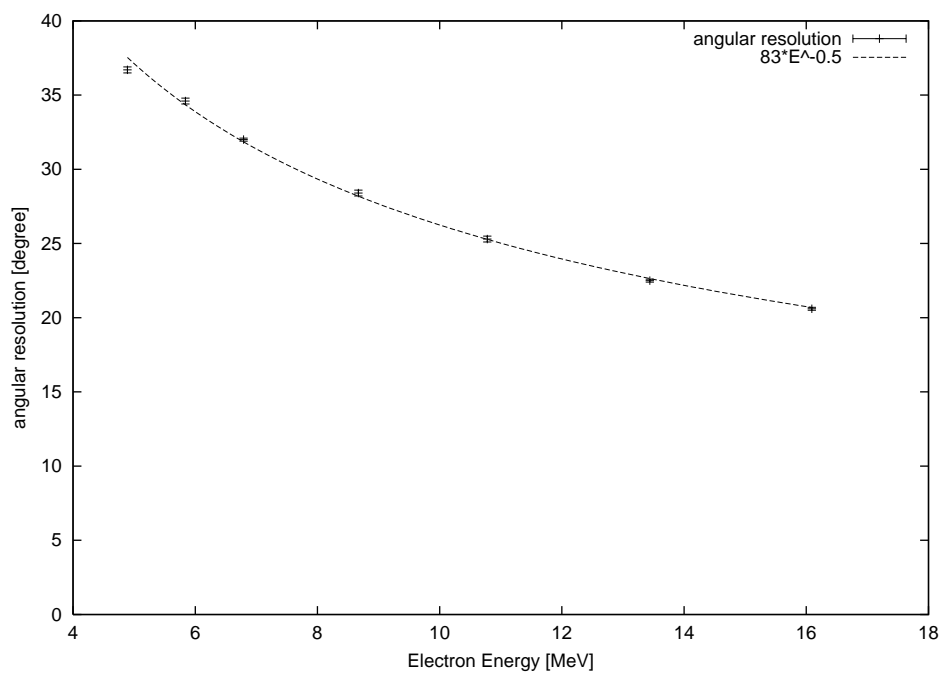


Figure 2: The angular resolution of SK detector. The dashed line is $83^\circ \times (E_e/\text{MeV})^{-1/2}$

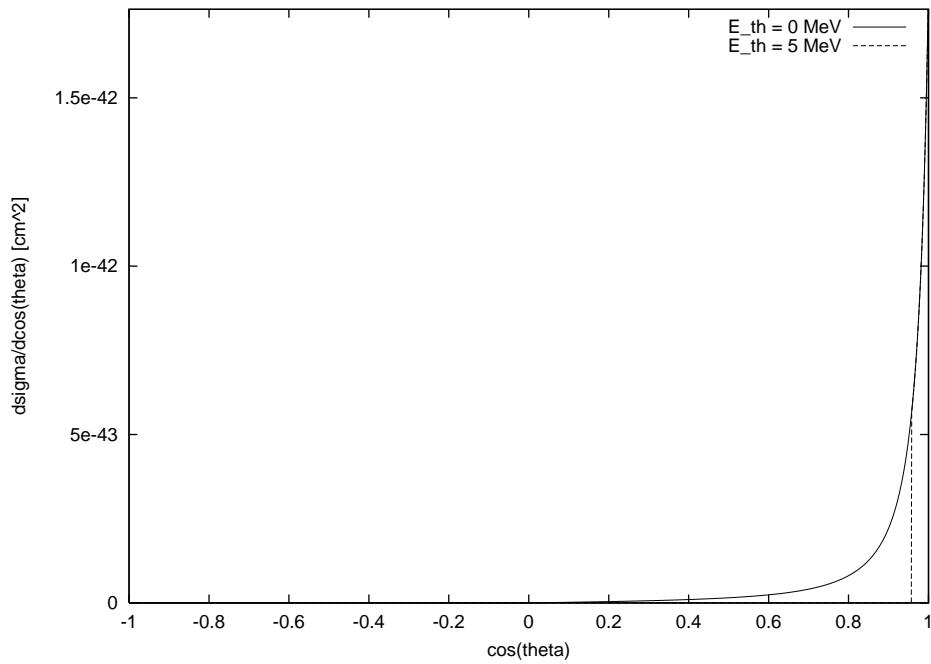


Figure 3: Cross section for $\nu_e + e^- \rightarrow \nu_e + e^-$. $E_\nu = 10$ MeV. The solid line is the cross section without an energy threshold. The dashed line is that with an energy threshold of 5 MeV, and that threshold is of SuperKamiokande detector. With the threshold, we can only see the event of $\cos \theta > 0.95$.

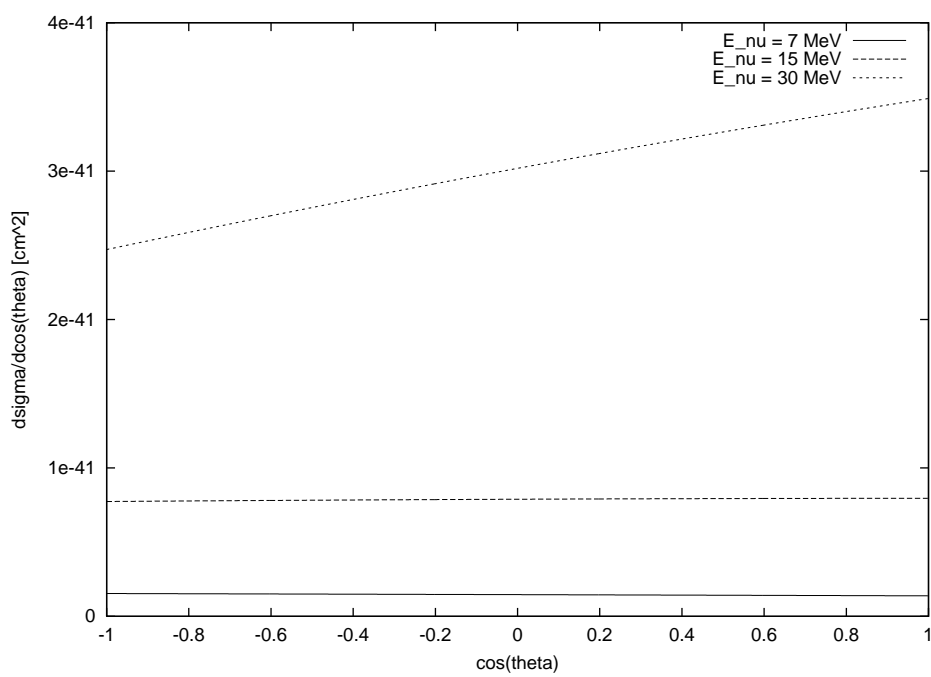


Figure 4: Cross sections for $\bar{\nu}_e + p \rightarrow e^+ + n$. These are almost isotropic. When $E_\nu = 30$ MeV, a weak forward peak can be seen, but this peak is not as sharp as scattering events.

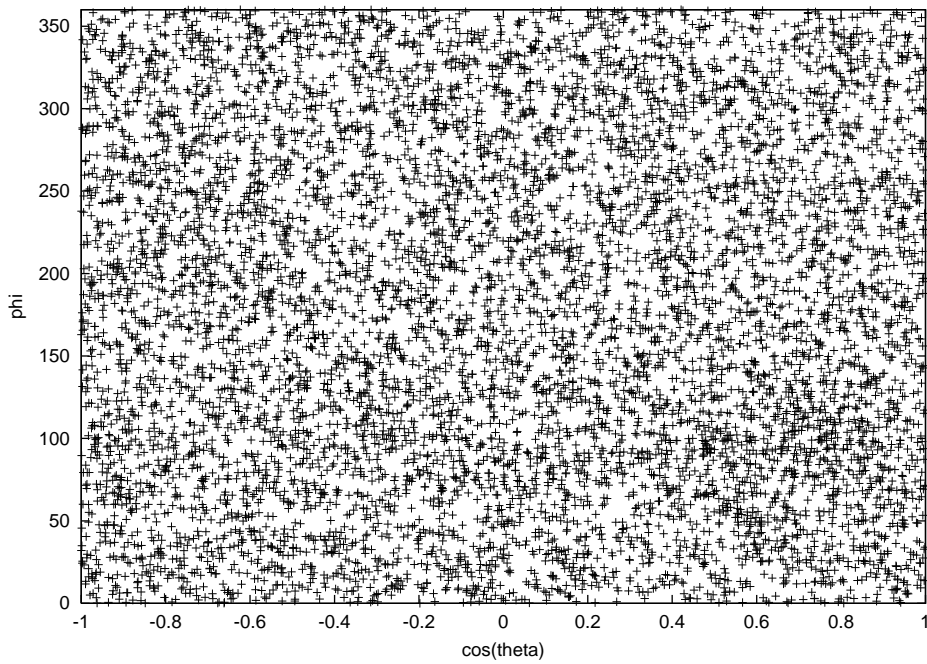


Figure 5: Events at SuperKamiokande detector. We see the obscure peak around $(\theta, \phi) \simeq (45^\circ, 90^\circ)$.

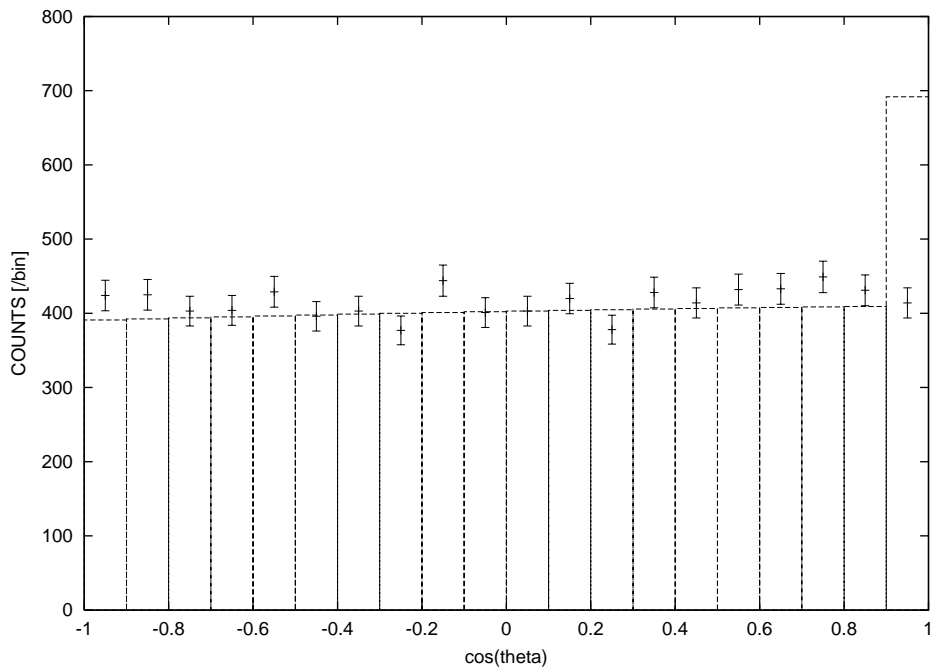


Figure 6: To analyze Fig. 5 result systematically, we divide $\cos \theta$ direction in 20 bins and sum up in each bin. This figure is the result of this operation. The dashed line is $\theta = 0^\circ$ peaked case, which can easily be calculated theoretically with cross sections.

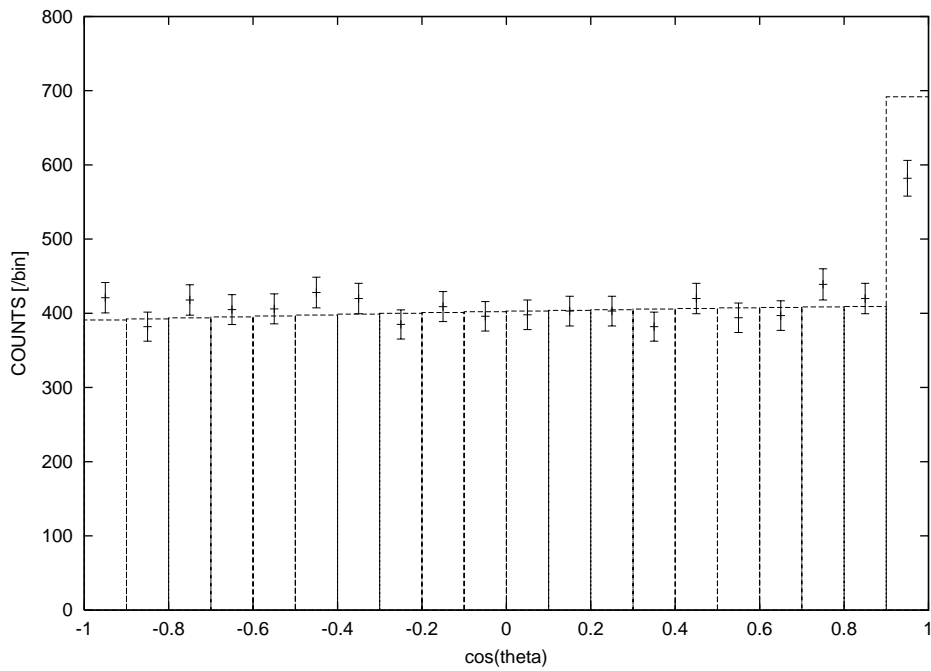


Figure 7: We rotate the coordinate for the events to be seen as in the case of $\theta = 0^\circ$ peaked by using the least-square method. This best-fitted result is obtained at coordinate rotation angle $(\theta, \phi) = (47.7^\circ, 80.0^\circ)$.

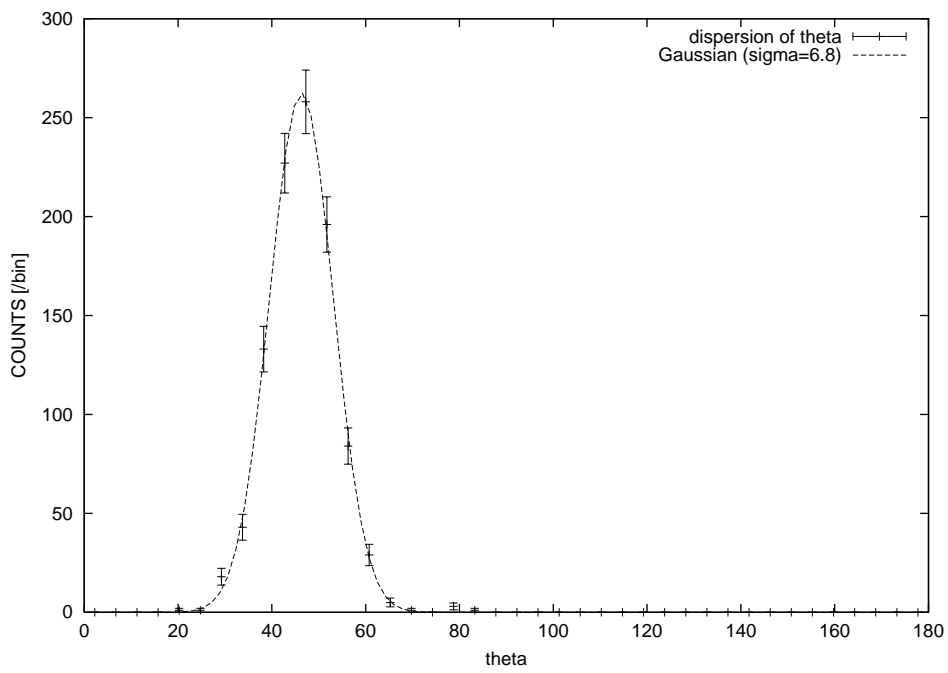


Figure 8: The distribution of best-fitted rotation angle θ . We fitted this result to Gaussian. $\theta_0 = 46.3^\circ, \delta\theta = 6.8^\circ$.

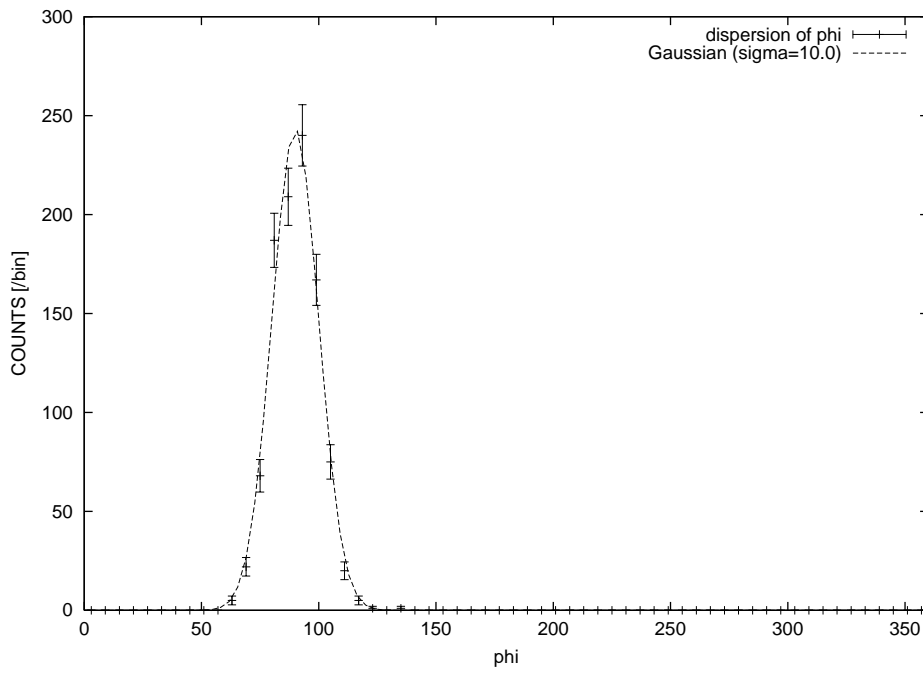


Figure 9: The distribution of best-fitted rotation angle ϕ . We fitted this result to Gaussian. $\phi_0 = 90.0^\circ$, $\delta\phi = 10.0^\circ$.

Table 1: Sets of mixing parameter for calculation

model	$\sin^2 2\theta_{12}$	$\sin^2 2\theta_{23}$	$\sin^2 2\theta_{13}$	$\Delta m_{12}^2(\text{eV}^2)$	$\Delta m_{13}^2(\text{eV}^2)$	ν_\odot problem
LMA-L	0.87	1.0	0.043	7.0×10^{-5}	3.2×10^{-3}	LMA
LMA-S	0.87	1.0	1.0×10^{-6}	7.0×10^{-5}	3.2×10^{-3}	LMA
SMA-L	5.0×10^{-3}	1.0	0.043	6.0×10^{-6}	3.2×10^{-3}	SMA
SMA-S	5.0×10^{-3}	1.0	1.0×10^{-6}	6.0×10^{-6}	3.2×10^{-3}	SMA

Table 2: Coefficients for cross section of $\nu e^- \rightarrow \nu e^-$. $g_V = 2 \sin^2 \theta_W - \frac{1}{2}$, $g_A = -\frac{1}{2}$, where θ_W is Weinberg angle.

coefficient	A	B	C
$\nu_e e^- \rightarrow \nu_e e^-$	$(g_V + g_A + 2)^2$	$(g_V - g_A)^2$	$(g_A + 1)^2 - (g_V + 1)^2$
$\bar{\nu}_e e^- \rightarrow \bar{\nu}_e e^-$	$(g_V - g_A)^2$	$(g_V + g_A + 2)^2$	$(g_A + 1)^2 - (g_V + 1)^2$
$\nu_{\mu,\tau} e^- \rightarrow \nu_{\mu,\tau} e^-$	$(g_V + g_A)^2$	$(g_V - g_A)^2$	$g_A^2 - g_V^2$
$\bar{\nu}_{\mu,\tau} e^- \rightarrow \bar{\nu}_{\mu,\tau} e^-$	$(g_V - g_A)^2$	$(g_V + g_A)^2$	$g_A^2 - g_V^2$

Table 3: Number of events at SuperKamiokande

model	LMA-L	LMA-S	SMA-L	SMA-S	no osc
$\bar{\nu}_e p$	9459	9427	8101	7967	8036
$\nu_e e^-$	186	115	189	131	132
$\bar{\nu}_e e^-$	46	46	41	42	42
$\nu_\mu e^-$	25	26	25	30	30
$\bar{\nu}_\mu e^-$	24	23	24	24	24
$\nu_\tau e^-$	25	26	25	30	30
$\bar{\nu}_\tau e^-$	24	23	24	24	24
$O\nu_e$	297	214	297	108	31
$O\bar{\nu}_e$	160	158	95	92	92
total	10245	10114	8822	8447	8441

Table 4: Best-fitted angles of coordinate rotation and these errors ($^\circ$)

model	LMA-L	LMA-S	SMA-L	SMA-S	no osc
θ_0	45.8	46.1	45.5	45.8	46.3
ϕ_0	89.7	89.9	90.4	90.0	90.0
$\delta\theta$	5.7	8.0	6.0	7.0	6.8
$\delta\phi$	7.9	11.0	7.8	9.1	10.0
σ	8.0	11.2	8.2	9.5	9.9